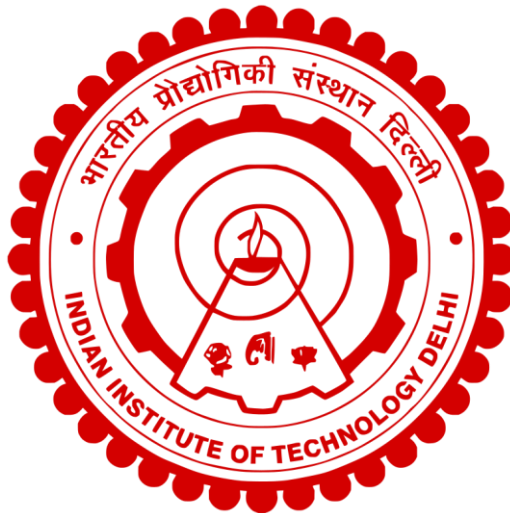


**DESIGN AND FABRICATION OF ELECTRO-OPTIC
DEVICES USING LIQUID CRYSTALS AND THEIR
INTEGRATION WITH POLYMERS**

RISHIKESH KUSHAWAHA



DEPARTMENT OF PHYSICS

INDIAN INSTITUTE OF TECHNOLOGY DELHI

JULY 2025

© Indian Institute of Technology Delhi (IITD), New Delhi, 2025

**DESIGN AND FABRICATION OF ELECTRO-OPTIC
DEVICES USING LIQUID CRYSTALS AND THEIR
INTEGRATION WITH POLYMERS**

by

RISHIKESH KUSHAWAHA

Department of Physics

submitted

in fulfillment of the requirements of the degree of Doctor of Philosophy

to the



INDIAN INSTITUTE OF TECHNOLOGY DELHI

JULY 2025

Dedicated to my Parents

CERTIFICATE

This is to certify that the thesis entitled, “**Design and fabrication of electro-optic devices using liquid crystals and their integration with polymers,**” being submitted by **Mr. Rishikesh Kushawaha** to the Indian Institute of Technology Delhi for the award of the degree of **Doctor of Philosophy** in Physics is a record of bonafide research work carried out by him. He has worked under my supervision and guidance and has fulfilled the requirements for the submission of this thesis, which to the best of my knowledge, has reached the requisite standard.

The contents of this thesis have not been submitted in part or in full to any other university or institute for the award of any degree or diploma.



14/July/2025

Prof. Aloka Sinha

Department of Physics

Indian Institute of Technology Delhi

Hauz Khas, New Delhi-110016

ACKNOWLEDGEMENT

I extend sincere thanks to all the individuals whose support and guidance have been essential in the completion of this thesis. I would like to express my heartfelt gratitude to my supervisor, Prof. Aloka Sinha, for her guidance and unwavering support, which have been essential to the successful completion of this work. I am thankful for her invaluable guidance, which has profoundly influenced my work and contributed to my growth. I am grateful for the time she dedicated to me, her understanding, and her constant belief in my abilities during uncertain times. I am thankful to her for giving me the freedom to explore my ideas, flexible working hours, encouraging me to take part in conferences and various academic events both inside and outside the institute, involving me in innovative projects, and always striving for excellence in my work.

Apart from my thesis supervisor, I express my sincere gratitude to the research committee members, Prof. D.S. Mehta (Department of Physics, IIT Delhi), Prof. P. Senthilkumaran (Department of Physics & Optics and Photonic Centre, IIT Delhi), and Prof. V. Haridas (Department of Chemistry, IIT Delhi), for their valuable time, insight and encouragement during the progress meetings.

I express my gratitude to our scientific collaborators, Prof. V. Haridas and Mr. Sagar Jawla, for the pseudopeptide polymer compound and for the insightful and comprehensive discussions regarding the work on the tunable light scattering device.

I acknowledge the nanoscale research facility (NRF), central research facility (CRF), Physics Department, and Chemistry Department of the institute for the characterization facilities. I would like to thank Prof. Sampa Saha (Department of Materials Science and Engineering, IIT Delhi) for the GPC facility. Ministry of Education, Government of India, and IIT Delhi are greatly acknowledged for providing the Ph.D. fellowship. I would also like to thank IIT Delhi

for providing financial assistance to attend the various conferences and workshops in India and abroad during my Ph.D.

I would like to express my thanks to all my lab mates; Dr. Pradeep Kumar, Dr. Amina Nafees, Dr. Susanta Chakraborty, Dr. Asha Kumari, Ms. Aysha Rani, Dr. Rahul Panchal, Ms. Shilpi Bose, Dr. Vaibhav Sharma, Mr. Deepak Verma, Mr. Dhananjoy Mandal, Mr. Kaustav Jit Bora, Mr. Debasish Bag, Mr. Harish Khan, Mr. Aman Mishra, Ms. Akriti, and Mr. Deepak Kararwal. Their assistance and support in both experimental and non-experimental work have been beneficial for me to complete this thesis.

I extend my heartfelt gratitude to my friends from IIT Delhi, including Dr. Himanshu Arora, Dr. Saurabh Pandey, Dr. Jamal Ahmad Khan, Dr. Rakesh Gangwar, Dr. Mohit, Mr. Roshan Singh and many others for their invaluable support, encouragement, and cherished companionship during my time away from the lab, both professionally and personally, throughout my doctoral journey.

My thesis is incomplete without expressing my sincere gratitude to my family members. I would like to take this opportunity to express my heartfelt appreciation to my family members who have been a significant source of support throughout this journey: my late grandfather, Sri Paras Nath Kushwaha, and my grandmother, Smt. Rampyari; my late great uncle, Shri Radha Krishna Kushwaha; my grand aunt, Smt. Kailashi; my father, Mr. Om Prakash Kushwaha; my mother, Smt. Mamta; my brother, Rakesh Kushwaha; my sister, Priyanka Kushwaha; my sister-in-law, Mrs. Prachi Priya Kushwaha; as well as my uncle, aunts, and cousins. I express my gratitude for their love, support, prayers, care, and well-wishes. Without their support, I would not have achieved the milestones that I have reached today.

July 2025

New Delhi

Rishikesh Kushwaha
14/July/2025
Rishikesh Kushawaha

ABSTRACT

Liquid crystal (LC) is a unique material, which has fluid-like behavior and also anisotropic properties. Their ability to exhibit anisotropy, birefringence, and fluid-like behavior has been utilized in several domains, like displays, optical systems, sensors, and biomedical devices. The nematic phase among the several mesophases of LCs provides greater dynamic control over the other mesophases. The development of novel LC variants featuring enhanced properties for various applications is an expensive and laborious process. Alternatively, to improve the properties of the nematic LC, the integration of nanoparticles and ionic medium in LCs has led to a modulation of the properties of the LC phases. This resulted in a reduction in threshold voltage and an improvement in response time. Furthermore, within the field of liquid crystalline materials, scientific research and technological progress have resulted in the emergence of novel concepts, one of which is the liquid crystal polymer composite.

The effective integration of LCs with polymers facilitates the emergence of various unique effects by adjusting the properties of the polymers and the LCs. LCPCs gained attention for the development of devices such as smart windows, advanced optical encryption, biosensors, flexible and foldable biosensors, energy harvesting devices, and numerous other innovations. The main categories of LCPCs are polymer-dispersed liquid crystals (PDLCs) and polymer-stabilized liquid crystals (PSLCs). PDLCs consist of liquid crystal droplets that range from micron to sub-micron sizes, which are integrated within a continuous polymer matrix. PSLCs incorporate a polymer stabilizing network within the continuous liquid crystal phase. In addition to PSLCs and PDLCs, the polymer exists in a ball/microsphere configuration within the liquid crystal category, classified as a polymer ball-filled liquid crystal. This thesis demonstrates the incorporation of the ionic medium in the LC and the development of the different kinds of LCPCs to fabricate devices such as free-standing optical diffuser, laser speckle contrast reducer, electrically tunable light scattering devices, and tunable phase grating,

which have potential applications in the field of electro-optics, foldable displays, and laser-based projection displays.

Chapter one covers the different phases of LCs, liquid crystal polymer composites (LCPCs), their classifications, and their physical properties. The light scattering in the different kinds of LC and LCPCs. Chapter two focuses on the fabrication of PDLC-based free-standing films, LC cells, and experimental methods to characterize the devices. Chapter three discusses the simple and straightforward approach for developing a free-standing film-based optical diffuser fabricated using 4'-Pentyl-4-biphenylcarbonitrile (5CB) nematic liquid crystals and cellulose acetate (CA) biopolymers. Films are fabricated using the solvent-induced phase separation approach. The films are foldable and show stronger light-scattering characteristics. In the films, a continuous cellulose acetate biopolymer network encapsulates micron and sub-micron LC droplets that scatter the light passing through the film. The films exhibit ultrahigh haze (~99%). The optimal concentration of LC with CA shows an angular transmission profile close to Lambertian distribution.

Chapter four investigates a nematic liquid crystal with negative dielectric anisotropy termed N-(4-Methoxybenzylidene)-4-Butylaniline (MBBA) doped with cetyltrimethylammonium bromide (CTAB) as a laser speckle contrast suppression device. Ionic medium cetyltrimethylammonium bromide (CTAB) increases ionic concentration, alters the dielectric properties, and improves electrohydrodynamic instability (EHDI). When light passes through the device, the EHDI effect produces dynamic scattering. Due to dynamic scattering, speckle patterns are generated. The speckle patterns are collected by a charge-coupled device (CCD) camera over a finite exposure time that is adequate to capture the phase modulation due to dynamic scattering. This results in a reduction in the speckle contrast. These investigations show that it reduces speckle contrast without a complicated setup.

Chapter Five covers the development of tunable light-scattering devices without the need for conventional UV or heat-curing methods. The polymer, composed of amino acid-based pseudopeptides, exhibits solvent-dependent self-assembling properties and is integrated into chiral nematic liquid crystals (CLC). In the E7 and CB15-based CLC, pseudopeptide polymer forms the micron-sized ball/sphere, which enhances the light scattering properties of the focal conic state of the CLC and reduces the threshold voltage. The 10 wt. % of the polymer in the CLC reduces the direct transmission twice compared to non-polymer CLC in the focal conic state. The inclusion of the polymer also improves the time required to induce the scattering state.

Chapter Six focuses on dielectric and light scattering properties of the pseudopeptide incorporated negative dielectric anisotropy nematic liquid crystal (nLC). In nLC, pseudopeptide polymer precipitates in the form of micrometer-sized spheres. Polymers enhance ion density, mobility, and conductivity, removing the need for an extra ionic medium to produce a stronger electrohydrodynamic instabilities (EHDI) state. The maximum ion density occurs with the 5 wt % polymer in the nLC, whereas higher values for the diffusion coefficient, ion mobility, and ac conductivity are observed with the 7.5 wt % polymer in the nLC. In the nLC with the pseudopeptide polymer microspheres, light scattering is significantly enhanced in the EHDI state. The pseudopeptide also provides an excellent contrast ratio and decreases the voltage required to produce a light-scattering state in the nLC.

Chapter Seven reports the one-dimensional (1D) and two-dimensional (2D) phase grating using the in-plane switching (IPLS) configuration of the LC cell with a nLC. Changing the orientation of nLC molecules between periodic electrode strips induces periodic refractive index variation. At the high frequency of the electric field, the device generates one-dimensional diffraction patterns that show voltage-dependent diffraction efficiencies in different orders. At low frequencies, it shows one-dimensional diffraction patterns at lower

voltage and two-dimensional in certain voltage ranges due to electroconvection rolls between the electrode strips.

The thesis concludes with a discussion of the future scope of the major results and the work presented in this thesis and their possible potential application in several electro-optic devices, such as projection displays, tunable optical diffusers, smart windows, beam steering, and foldable optical technology.

लिक्विड क्रिस्टल (एलसी) एक अद्वितीय पदार्थ है, जिसका व्यवहार तरल पदार्थ जैसा होता है तथा इसमें अनिसोट्रोपिक गुण भी होते हैं। अनिसोट्रॉपी, द्विअपवर्तन और द्रव जैसा व्यवहार प्रदर्शित करने की उनकी क्षमता का उपयोग कई क्षेत्रों में किया गया है, जैसे डिस्प्ले, ऑप्टिकल सिस्टम, सेंसर और बायोमेडिकल डिवाइस। एलसी के कई मध्यावस्थाओं के बीच नेमैटिक चरण अन्य मध्यावस्थाओं पर अधिक गतिशील नियंत्रण प्रदान करता है। विभिन्न अनुप्रयोगों के लिए उन्नत गुणों की विशेषता वाले नए LC वेरिएंट का विकास एक महंगी और श्रमसाध्य प्रक्रिया है। वैकल्पिक रूप से, नेमैटिक LC के गुणों को बेहतर बनाने के लिए, LC में नैनोकणों और आयनिक माध्यम के एकीकरण ने LC चरणों के गुणों के मॉड्यूलेशन को जन्म दिया है। इसके परिणामस्वरूप थ्रेशोल्ड वोल्टेज में कमी आई और प्रतिक्रिया समय में सुधार हुआ। इसके अलावा, लिक्विड क्रिस्टलीय सामग्रियों के क्षेत्र में, वैज्ञानिक अनुसंधान और तकनीकी प्रगति के परिणामस्वरूप नई अवधारणाएँ सामने आई हैं, जिनमें से एक लिक्विड क्रिस्टल पॉलीमर कंपोजिट है।

पॉलिमर के साथ LCs का प्रभावी एकीकरण पॉलिमर और LCs के गुणों को समायोजित करके विभिन्न अनूठे प्रभावों के उद्भव की सुविधा प्रदान करता है। LCPC ने स्मार्ट विंडो, उन्नत ऑप्टिकल एन्क्रिप्शन, बायोसेंसर, लचीले और फोल्डेबल बायोसेंसर, ऊर्जा संचयन उपकरण और कई अन्य नवाचारों जैसे उपकरणों के विकास के लिए ध्यान आकर्षित किया। LCPC की मुख्य श्रेणियां पॉलिमर-फैलाए गए लिक्विड क्रिस्टल (PDLC) और पॉलिमर-स्थिर लिक्विड क्रिस्टल (PSLC) हैं। PDLC में लिक्विड क्रिस्टल की बूंदें होती हैं जो माइक्रोन से लेकर सब-माइक्रोन आकार तक होती हैं, जिन्हें एक सतत पॉलिमर मैट्रिक्स के भीतर एकीकृत किया जाता है। PSLCs में सतत लिक्विड क्रिस्टल चरण के भीतर एक पॉलिमर स्थिरीकरण नेटवर्क शामिल होता है। PSLCs और PDLCs के अलावा, पॉलिमर लिक्विड क्रिस्टल श्रेणी के भीतर एक बॉल/माइक्रोस्फीयर विन्यास में मौजूद होता है, जिसे पॉलिमर बॉल-फिल्ड लिक्विड क्रिस्टल के रूप में वर्गीकृत किया जाता है। यह शोध प्रबंध एलसी में आयनिक माध्यम के समावेश और विभिन्न

प्रकार के एलसीपीसी के विकास को प्रदर्शित करता है, जिससे फ्री-स्टैंडिंग ऑप्टिकल डिफ्यूजर, लेजर स्पेकल कॉन्ट्रास्ट रिड्यूसर, विद्युत रूप से ट्यूनेबल लाइट स्कैटरिंग डिवाइस और ट्यूनेबल फेज ग्रेटिंग जैसे उपकरणों का निर्माण किया जा सके, जिनके इलेक्ट्रो-ऑप्टिक्स, फोल्डेबल डिस्प्ले और लेजर-आधारित प्रोजेक्शन डिस्प्ले के क्षेत्र में संभावित अनुप्रयोग हैं।

अध्याय एक में LCs, लिक्विड क्रिस्टल पॉलीमर कंपोजिट (LCPCs), उनके वर्गीकरण और उनके भौतिक गुणों के विभिन्न चरणों को शामिल किया गया है। विभिन्न प्रकार के LC और LCPC में प्रकाश का प्रकीर्णन। अध्याय दो PDLC-आधारित मुक्त-स्थायी फिल्मों, LC कोशिकाओं और उपकरणों की विशेषता बताने के लिए प्रयोगात्मक तरीकों के निर्माण पर केंद्रित है। अध्याय तीन में 4'-पेंटाइल-4-बाइफेनिलकार्बोनाइट्राइल (5CB) नेमैटिक लिक्विड क्रिस्टल और सेल्यूलोज एसीटेट (CA) बायोपॉलिमर का उपयोग करके निर्मित एक मुक्त-स्थायी फिल्म-आधारित ऑप्टिकल डिफ्यूजर विकसित करने के लिए सरल और सीधे दृष्टिकोण पर चर्चा की गई है। विलायक-प्रेरित चरण पृथक्करण दृष्टिकोण का उपयोग करके फिल्मों का निर्माण किया जाता है। फिल्में फोल्डेबल हैं और मजबूत प्रकाश-प्रकीर्णन विशेषताएँ दिखाती हैं। फिल्मों में, एक सतत सेल्यूलोज एसीटेट बायोपॉलिमर नेटवर्क माइक्रोन और सब-माइक्रोन LC बूंदों को समाहित करता है जो फिल्म से गुजरने वाले प्रकाश को बिखेरते हैं। फिल्में अल्ट्राहाई धुंध (~ 99%) प्रदर्शित करती हैं। सीए के साथ एलसी की इष्टतम सांद्रता लैम्बर्टियन वितरण के करीब एक कोणीय संचरण प्रोफ़ाइल दिखाती है।

अध्याय चार में एक नेमैटिक लिक्विड क्रिस्टल की जांच की गई है जिसमें नकारात्मक डाइइलेक्ट्रिक अनिसोट्रॉपी है जिसे N-(4-मेथॉक्सीबेंज़िलिडीन)-4-ब्यूटाइलएनिलिन (MBBA) कहा जाता है जिसे लेजर स्पेकल कंट्रास्ट सप्रेसन डिवाइस के रूप में सीटाइलट्राइमेथाइलमोनियम ब्रोमाइड (CTAB) के साथ डोप किया गया है। आयनिक माध्यम सीटाइलट्राइमेथाइलमोनियम ब्रोमाइड (CTAB) आयनिक सांद्रता को बढ़ाता है, डाइइलेक्ट्रिक गुणों को बदलता है, और इलेक्ट्रोहाइड्रोडायनामिक अस्थिरता (EHDI) में सुधार

करता है। जब प्रकाश डिवाइस से होकर गुजरता है, तो EHD प्रभाव गतिशील प्रकीर्णन पैदा करता है। गतिशील बिखराव के कारण, धब्बेदार पैटर्न उत्पन्न होते हैं। धब्बेदार पैटर्न को एक चार्ज-युग्मित डिवाइस (सीसीडी) कैमरे द्वारा एक सीमित एक्सपोजर समय पर एकत्र किया जाता है जो गतिशील बिखराव के कारण चरण मॉड्यूलेशन को पकड़ने के लिए पर्याप्त है। इसके परिणामस्वरूप धब्बेदार कंट्रास्ट में कमी आती है। ये जांच दर्शाती है कि यह जटिल सेटअप के बिना धब्बेदार कंट्रास्ट को कम करता है।

अध्याय पाँच में पारंपरिक UV या ताप-उपचार विधियों की आवश्यकता के बिना ट्यूनेबल प्रकाश-प्रकीर्णन उपकरणों के विकास को शामिल किया गया है। अमीनो एसिड-आधारित स्यूडोपेप्टाइड्स से बना पॉलिमर, विलायक-निर्भर स्व-संयोजन गुणों को प्रदर्शित करता है और इसे चिरल नेमेटिक लिक्विड क्रिस्टल (CLC) में एकीकृत किया जाता है। E7 और CB15-आधारित CLC में, स्यूडोपेप्टाइड पॉलिमर माइक्रोन आकार की गेंद/गोला बनाता है, जो CLC की फ़ोकल शंकु अवस्था के प्रकाश प्रकीर्णन गुणों को बढ़ाता है और थ्रेशोल्ड वोल्टेज को कम करता है। CLC में पॉलिमर का 10 wt. % फ़ोकल शंकु अवस्था में गैर-पॉलिमर CLC की तुलना में प्रत्यक्ष संचरण को दोगुना कम करता है। पॉलिमर को शामिल करने से प्रकीर्णन अवस्था को प्रेरित करने के लिए आवश्यक समय में भी सुधार होता है।

अध्याय छह में स्यूडोपेप्टाइड के डाइइलेक्ट्रिक और प्रकाश प्रकीर्णन गुणों पर ध्यान केंद्रित किया गया है, जिसमें नेगेटिव डाइइलेक्ट्रिक अनिसोट्रॉपी नेमेटिक लिक्विड क्रिस्टल (nLC) शामिल है। nLC में, स्यूडोपेप्टाइड पॉलिमर माइक्रोमीटर आकार के गोले के रूप में अवक्षेपित होता है। पॉलिमर आयन घनत्व, गतिशीलता और चालकता को बढ़ाते हैं, जिससे एक मजबूत इलेक्ट्रोहाइड्रोडायनामिक अस्थिरता (EHD) स्थिति उत्पन्न करने के लिए अतिरिक्त आयनिक माध्यम की आवश्यकता समाप्त हो जाती है। nLC में 5 wt % पॉलिमर के साथ अधिकतम आयन घनत्व होता है, जबकि nLC में 7.5 wt % पॉलिमर के साथ प्रसार गुणांक, आयन गतिशीलता और ac चालकता के लिए उच्च मान देखे जाते हैं। स्यूडोपेप्टाइड पॉलिमर माइक्रोस्फीयर के साथ nLC में, EHD अवस्था में प्रकाश प्रकीर्णन काफी बढ़ जाता है।

स्यूडोपेराइड एक उत्कृष्ट कंट्रास्ट अनुपात भी प्रदान करता है और nLC में प्रकाश-प्रकीर्णन अवस्था उत्पन्न करने के लिए आवश्यक वोल्टेज को कम करता है।

अध्याय सात में एनएलसी के साथ एलसी सेल के इन-प्लेन स्विचिंग (आईपीएलएस) कॉन्फ़िगरेशन का उपयोग करके एक-आयामी (1डी) और दो-आयामी (2डी) चरण झंझरी की रिपोर्ट दी गई है। आवधिक इलेक्ट्रोड स्ट्रिप्स के बीच एनएलसी अणुओं के अभिविन्यास को बदलने से आवधिक अपवर्तक सूचकांक भिन्नता उत्पन्न होती है। विद्युत क्षेत्र की उच्च आवृत्ति पर, उपकरण एक-आयामी विवर्तन पैटर्न उत्पन्न करता है जो विभिन्न क्रमों में वोल्टेज-निर्भर विवर्तन दक्षताओं को दर्शाता है। कम आवृत्तियों पर, यह कम वोल्टेज पर एक-आयामी विवर्तन पैटर्न और इलेक्ट्रोड स्ट्रिप्स के बीच इलेक्ट्रो-कन्वेक्शन रोल के कारण कुछ वोल्टेज श्रेणियों में दो आयामी दिखाता है।

थीसिस का समापन इस थीसिस में प्रस्तुत प्रमुख परिणामों और कार्य के भविष्य के दायरे और कई इलेक्ट्रो-ऑप्टिक उपकरणों, जैसे कि प्रोजेक्शन डिस्प्ले, ट्यूनेबल ऑप्टिकल डिफ्यूज़र, स्मार्ट विंडो, बीम स्टीयरिंग और फोल्डेबल ऑप्टिकल टेक्नोलॉजी में उनके संभावित अनुप्रयोग की चर्चा के साथ हुआ।

TABLE OF CONTENTS

CERTIFICATE	i
ACKNOWLEDGMENT	ii
ABSTRACT	iv
संर	viii
TABLE OF CONTENT	xii
TABLE OF FIGURES	xvi
LIST OF TABLES	xxii
LIST OF ABBREVIATIONS	xxiii
LIST OF SYMBOLS	xxiv
Chapter One: Introduction	1
1.1 Brief history of liquid crystals.....	1
1.2 Classification of the liquid crystals	3
1.2.1 Thermotropic liquid crystals.....	3
1.2.1.1 Nematic liquid crystals	4
1.3 Physical properties of the nematic liquid crystals.....	6
1.3.1 Order parameter.....	6
1.3.2 Dielectric anisotropy.....	7
1.3.3 Optical anisotropy (Birefringence).....	8
1.3.4 Elastic properties	9
1.3.5 Freedericksz transition.....	10
1.4 Dispersion of the ionic medium in the LCs.....	12
1.5 Liquid crystal polymer composites (LCPCs).....	12
1.5.1 Classification of the liquid crystal polymer composites.....	14
1.5.1.1 Polymer-dispersed liquid crystals (PDLCs).....	14
1.5.1.2 Polymer-stabilized liquid crystals (PSLCs)	16
1.5.1.3 Polymer ball/microsphere-filled liquid crystals (PFLCs).....	17
1.5.2 Properties of the LCPCs	18
1.5.2.1 Light scattering in the LCPCs.....	18
1.6 Light scattering in the cholesteric LC	20
1.7 Light diffraction and scattering due to electroconvection and electrohydrodynamic instabilities in the nematic liquid crystals	20
1.8 Parameters for characterization of the light scattering.....	22
1.8.1 Direct transmission	22
1.8.2 Total transmission and Haze	22

1.8.3 Contrast ratio	23
1.8.4 Response time.....	23
1.8.5 Switching voltages.....	23
1.9 Application of the electroconvection and electrohydrodynamic instabilities	24
1.9.1 Diffraction grating	24
1.9.2 Laser speckle contrast suppression.....	24
1.10 Motivation	25
1.11 Objectives of the thesis.....	26
1.12 Organization of the thesis.....	27
Reference.....	34
Chapter Two: Experimental methods and techniques	38
2.1 Free-standing film preparation of the liquid crystal and polymers	38
2.2 Liquid crystal cell fabrication	39
2.2.1 Pattern formation on the indium tin oxide (ITO) coated glass substrate.....	40
2.2.2 Fabrication of the homogeneous LC cell.....	41
2.2.3 Homeotropic LC cell preparation	42
2.3 Characterization of the LC-based devices.....	42
2.3.1 Thermal characterizations.....	42
2.3.1.1 Thermogravimetric analysis (TGA).....	42
2.3.2 Morphological characterizations	44
2.3.2.1 Polarizing optical microscope.....	44
2.3.2.2 Scanning electron microscope (SEM) and Field scanning electron microscope (FESEM).....	47
2.3.2.3 Atomic force microscopy (AFM).....	49
2.3.3 Angular transmission	50
2.3.4 Laser speckle contrast measurement	51
2.3.5 UV-visible spectrometer for total transmittance and haze.....	53
2.3.6 Electro-optic characterization.....	54
2.3.7 Dielectric spectroscopy.....	55
2.4 Error analysis and precision of the instruments	57
References	60
Chapter Three: Fabrication of the foldable free-standing optical diffuser based on polymer-dispersed liquid crystals.....	62
3.1 Introduction	62
3.2 Experimental details	64
3.2.1 Materials and fabrication	64
3.2.2 Thickness and Morphologies of films	65
3.2.3 Optical characterization.....	66

3.2.3.1 Angular transmittance measurement.....	66
3.2.3.2 Transmittance and haze of films	67
3.3 Results and Discussion.....	67
3.4 Conclusion.....	73
References	74
Chapter Four: Suppression of the laser speckle contrast using the electro-hydrodynamic instabilities in the negative dielectric anisotropy liquid crystal incorporated with an ionic medium	76
4.1 Introduction.....	76
4.2 Material and fabrication	79
4.3 Experimental details.....	79
4.4 Results and Discussion.....	81
4.4.1 Optical texture	81
4.4.2 Optical transmission	83
4.4.3 Speckle contrast measurement.....	85
4.4.4 Intensity profile of the speckle images	88
4.4.5 Dielectric spectroscopy.....	89
4.5 Conclusion.....	94
References	95
Chapter Five: Fabrication of the tunable light scattering device using the pseudopeptide polymer microsphere/ball precipitation in chiral nematic liquid crystal	97
5.1 Introduction	97
5.2 Materials and Methods	99
5.2.1 Sample preparation	99
5.2.2 Cell fabrication	100
5.3 Characterization details	100
5.4 Results and Discussion.....	102
5.5 Conclusion.....	116
References	117
Chapter Six: Fabrication of the tunable light scattering device using electrohydrodynamic instabilities and pseudopeptide polymer microsphere in the negative dielectric anisotropic nematic liquid crystal	120
6.1 Introduction	120
6.2 Materials and sample preparation	123
6.3 Characterization details	123

6.4 Result and Discussion	124
6.4.1 Dielectric spectroscopy.....	125
6.4.2 Electro-optic analysis	133
6.4.2.1 Optical texture.....	133
6.4.2.2 Transmission studies	136
6.5 Conclusion.....	142
References	142
Chapter Seven: Tunable one-dimensional and two-dimensional diffraction phase grating using negative dielectric anisotropy liquid crystal.....	145
7.1 Introduction	145
7.2 Device fabrication	146
7.3 Experimental details	147
7.4 Result and Discussion	148
7.5 Conclusion.....	155
Reference.....	156
Chapter Eight: Conclusion and future scope	157
8.1 Conclusion of the work	157
8.2 Future scope	160
Appendix A	162
Appendix B	169
Appendix C	172
Publications	175
Published work in journals.....	175
Manuscript under preparation	175
Conferences.....	175
Workshop	176
AUTHOR'S BIOGRAPHY	177

TABLE OF FIGURES

Figure 1. 1 Classification of the liquid crystals.....	2
Figure 1. 2 Thermotropic LC phase as the function of the temperature variation	3
Figure 1. 3 (a) Nematic and (b) cholesteric LC phase formed by the calamitic LC	5
Figure 1. 4 Schematic of the orientation of the LC molecules.....	6
Figure 1. 5 (a) The refractive index of the calamitic nematic LC along the long and short axis, (b) when the long axis (optic-axis) makes an angle with light propagation direction.	9
Figure 1. 6 (a) splay, (b) twist, and (c) bend deformation in the liquid crystals	9
Figure 1. 7 Schematic of the (a-c) homogeneous aligned LC cell filled with positive dielectric anisotropy LC, (d-f) homeotropic aligned LC cell filled with negative dielectric anisotropy LC	11
Figure 1. 8 (a) Light scattering from PDLC film, (b,c) PDLC's droplet configurations	15
Figure 1. 9 Schematic of the PSLC cell without any substrate treatment (a) off state, (b) on state	17
Figure 1. 10 The schematic of the CLC-based PFLC device in (a) off state, (b) focal conic state, and (c) homeotropic state	18
Figure 2. 1 Schematic of the LCPC-based free-standing film preparation.....	39
Figure 2. 2 Different steps of photolithography for pattern transfer and ITO etching.....	41
Figure 2. 3 (a) Component of the TGA instrument, (b) Image of the instrument.....	43
Figure 2. 4 (a) Photograph of the POM, (b) Schematic of the uniformly aligned LC molecules between crossed polarizers	45
Figure 2. 5 Photograph of voltage-dependent optical texture characterization setup.....	47
Figure 2. 6 (a) Schematic of FESEM working, (b) electron-matter interaction and type of signal generated, (c) photograph of TESCAN Magna instrument	48

Figure 2. 7 (a) Schematic of the AFM working, (b) Photograph of the Oxford instruments AFM	50
Figure 2. 8 (a) Schematic of the angular transmission setup, (b) Photograph of the setup	51
Figure 2. 9 (a) Schematic of the objective speckle setup, (b) Photograph of the setup	52
Figure 2. 10 (a) Image of the setup, (b) Schematic of the integrating sphere	53
Figure 2. 11 (a) Schematic of the direct transmission setup, (b) Photograph of the setup.....	54
Figure 2. 12 Photograph of the dielectric measurement setup	56
Figure 3. 1 Photograph of the 45 wt % LC film in front of a background (a). Film in the normal position (b). Film in the folded position	65
Figure 3. 2 Photographs of the diffused light of He-Ne laser beam $\lambda=633$ nm on the screen for (a). CA film, (b). 45 wt % LC/CA film, (c). 55 wt % LC/CA film, (d). 65 wt % LC/CA film. The image of the direct laser beam on the screen is shown in the lower left of each photograph. The length of the scale bar in white in Figure (a) is 2 cm. (e). Schematic set up to record photographs of the diffused light on the white paper screen.	66
Figure 3. 3 SEM images of the LC/CA films of (a). CA film, (b). 45 wt % LC/CA film, (c). 55 wt % LC/CA film, (d). 65 wt % LC/CA film, right upper corner of the images (b-d) is the distribution of pore diameter.....	67
Figure 3. 4 Angular distribution of the transmitted laser beam for (a). CA film, (b). 45 wt % LC/CA film, (c). 55 wt % LC/CA film, (d). 65 wt % LC/CA film, (e). for the 45, 55, and 65 wt % LC/CA, film. (f). FWHM of the angular transmitted plot.....	69
Figure 3. 5 Transmittance and Haze of (a). CA film, and 55 wt % LC/CA film, (b). 45 wt % and 65 wt % LC/CA film.	71
Figure 3. 6 Image (a) and (b) is the 55 wt % LC/CA film for different bending circles, (c) angular transmission plot for different bending circles, (d). FWHM for the different bending positions.....	72

Figure 4. 1 Photograph of 0.1 wt % CTAB doped MBBA LC Cell (a). without external voltage, (b). for $V_{pp} = 60$ Volt at $f = 50$ Hz. The square dashed area is the electrode region of the cell. The length of the scale bar in Figure (a) is 1 cm.81

Figure 4. 2 POM texture image of 0.1 wt % CTAB doped MBBA LC cell corresponding to different applied voltage and frequency of the applied square waveform. The polarizer (P) and analyzer(A) are in a cross position for all the images. It is shown only corresponding to $V_{pp} = 0$ for each frequency. The spherical dot in the images is the spacer beads present in the cell. 82

Figure 4. 3 Direct transmittance of the sample for 50 Hz operating frequency, and (b). for 0.1 wt % CTAB doped LC cell for different frequency and voltage. (c). schematic diagram when the laser beam passes through the LC cell (i) without and (ii) with the application of an electric field to produce the EHDI effect in the LC cell.84

Figure 4. 4 Flow chart of the steps for post-processing data85

Figure 4. 5 (a). The color map of the speckle contrast corresponds to the different amplitude of the applied voltage for $f = 50$ Hz of the CTAB doped LC systems (b). Color map of speckle contrast for 0.1 wt % CTAB doped MBBA LC system corresponding to the different frequencies.86

Figure 4. 6 Speckle contrast of 0 and 0.1 wt % CTAB doped LC cell for different applied voltage at a different frequency, (b) Speckle contrast of 0.1 wt % CTAB doped LC cell with different exposure time of the CCD camera.87

Figure 4. 7 CCD image of the 0.1 wt % CTAB doped MBBA LC cell at the different applied voltage for $f = 50$ Hz at $27\text{ }^{\circ}\text{C}$, and line profile of intensity across the horizontal central line.88

Figure 4. 8 Speckle Contrast value of 0.1 wt % CTAB doped LC cell over the number of days. The measurement's temperature value is $T = 27\text{ }^{\circ}\text{C}$89

Figure 4. 9 Dielectric spectroscopy, ion density, diffusion constant, and ac conductivity of the LC cells at 27 °C.	90
Figure 4. 10 (a) Dielectric spectroscopy, (b) ion density, and diffusion constant of 0.1 wt % CTAB doped LC at different temperatures. (c). Ion mobility graph of LC at 27 °C (d). ion mobility graph of 0.1 wt % CTAB doped MBBA LC corresponding to different temperature.	92
Figure 5. 1 (a). Chemical structure of Exo-norbornene Phe-OMe (NBFOMe) polymer, (b). FTIR spectroscopy of the E7 LC, NBFOMe polymer, and polymer after washing the LC from sample.	103
Figure 5. 2 Optical texture of the LC cells with different wt.% of the polymer at different voltages for $f = 1\text{kHz}$. Crossed double sided arrows represent the polarizer and analyzer. ..	104
Figure 5. 3 FESEM and AFM image of the (a ₁ - a ₃). 5 wt. % and (b ₁ - b ₃). 10 wt. % polymer content LC cell.....	106
Figure 5. 4 The direct transmission of the He-Ne laser beam passes through the LC cell at (a) 0P polarization, (b) 90P polarization state for different voltage amplitude at 1 kHz frequency.	107
Figure 5. 5 Photograph of 90:10 wt % CLC and polymer LC cell and schematic diagram of LC molecular arrangement, (a & d) Planer state at $V_{pp} = 0\text{ V}$, (b & e) focal conic state at $V_{pp} = 11\text{ V}$, and (c & f) Homeotropic state at $V_{pp} = 50\text{ V}$. Frequency $f = 1\text{ kHz}$. dashed area is filled with the sample.	108
Figure 5. 6 Wavelength-dependent direct transmission of the LC cells with 0wt. %, 5wt.% and 10 wt. % polymer.	112
Figure 5. 7 The light diffusion of the He-Ne laser beam passes through the LC cell with different polymer wt.% at different voltages for 1 kHz frequency. The scale in the Figure is 2 cm.....	113

Figure 5. 8 Response time data of the LC cells.	115
Figure 6. 1 FESEM image and polymer sphere size distribution of (a,d) 2.5 wt. % polymer, (b,e) 5 wt. % polymer, (c,f) 7.5 wt. % Polymer in the nLC.....	125
Figure 6. 2 Frequency dependence ϵ' , ϵ'' and $\tan\delta$ plot of (a,b,c) nLC alone, (d,e,f) 2.5 wt. % polymer in nLC, (g,h,i) 5 wt. % polymer in nLC, (j,k,l) 7.5 wt. % polymer in nLC at different temperatures.....	128
Figure 6. 3 (a) Dielectric data of 5 wt. % polymer in nLC with the fitted data at 30 °C, (b) ion density of all the four samples at different temperatures, (c) diffusion coefficient vs temperature, (d) ion mobility vs temperature.	131
Figure 6. 4 AC conductivity of the (a) LC alone, (b) 2.5 wt. %, (c) 5 wt. % polymer and (d) 7.5 wt. % polymer in nLC.....	132
Figure 6. 5 Optical texture micrograph of the nLC with different wt. % of the polymer at different voltages for $f = 50$ Hz and $T = 30$ °C.	134
Figure 6. 6 Direct transmission of the LC cells with (a,b) nLC alone, (c,d) 2.5 wt. % polymer in nLC, (e,f) 5 wt. % polymer in the nLC, (g,h) 7.5 wt. % polymer in nLC.	138
Figure 6. 7 Light scattering image of the laser beam from different LC cells at different voltage amplitude corresponding to the 50 Hz frequency and $T = 30$ °C. The scale bar is given in the 0wt. % polymer LC cell pattern at 0 V is 2 cm.....	139
Figure 6. 8 Photograph of the 5 wt. % polymer LC cell at (a) 0 V, (b) 60 V, for $f = 50$ Hz. The dimension of the square box in the dashed line is 1×1 cm ²	140
Figure 6. 9 Response time measurement of the different LC cells at 50 Hz and $V_{pp} = 60$ V. (a,b) Variation in intensity as the voltage is applied and removed, (c) Rise and fall time data, (d) contrast ratio as a function of polymer concentration in nLC for 50 Hz frequency	141
Figure 7. 1 Schematic diagram of the set-up to record the power in different diffraction orders	147

Figure 7. 2 Schematic of the (a) IPS electrodes, (b) LC cell without voltage, (c) with the voltage. The dotted curve represents the electric field lines. 148

Figure 7. 3 Optical texture corresponds to the different voltage amplitude at 1kHz. P and A represent the polarizer and analyzer. The scale bar is the same for all images..... 149

Figure 7. 4 Diffraction patterns at 1kHz for different voltage amplitude. The yellow box shows zeroth order 150

Figure 7. 5 Voltage-dependent diffraction efficiency of (a) 0P and (b) 90P polarization at 1kHz 151

Figure 7. 6 Optical texture corresponds to the different voltage amplitude at 20Hz 152

Figure 7. 7 Diffraction patterns at 20Hz for different voltage amplitude. The yellow box represents zeroth order 153

Figure 7. 8 Voltage-dependent diffraction efficiency of (a) 0P, (b) 90P polarization, and (c) 2D diffraction patterns at 20Hz 153

Figure 7. 9 Diffraction patterns correspond to the 35 Hz and 50 Hz at different voltages ... 154

Figure 7. 10 Response time data for (a) second order at 1kHz, and (b) fourth order at 20 Hz 155

LIST OF TABLES

Table 3.1 Compositions of the films	65
Table 3.2 Transmittance, Haze and FWHM of the films.....	68
Table 4.1 Minimum voltage (peak-to-peak in Volt) to start the EHDI effect for different frequencies.....	83
Table 4.2 Ion density, diffusion constant, and ion mobility of the LC at 27 °C.....	91
Table 5.1 LC and polymer content of different samples.....	100
Table 6.1 Activation energy of the nLC with different concentration of the NBFOMe polymer.....	130

LIST OF ABBREVIATIONS

LC: Liquid crystal	IPS: In-plane switching
CLC: Chiral nematic or cholesteric LC	POM: Polarizing optical microscope
CTAB: Cetrimonium bromide	5CB: 4'-Pentyl-4-biphenylcarbonitrile
EHDI: Electrohydrodynamic instabilities	MBBA: N-(4-Methoxybenzylidene)-4-butylaniline
LCPC: Liquid crystal polymer composite	nLC: Negative dielectric anisotropy nematic LC
SIPS: Solvent-induced phase separation	IPA: Isopropyl alcohol
TIPS: Temperature-induced phase separation	DI: Deionized
PIPS: Polymerization-induced phase separation	ITO: Indium tin oxide
P-PIPS: Photo-induced PIPS	PR: Photoresist
T-PIPS: Thermally initiated PIPS	TGA: Thermogravimetric analysis
PDLC: Polymer-dispersed liquid crystal	SEM: Scanning electron microscope
PSLC: Polymer-stabilized liquid crystal	FESEM: Field scanning SEM
PFLC: Polymer ball/microsphere-filled liquid crystal	AFM: Atomic force microscope
EC: Electroconvection	OD: Optical diffuser
C.R.: Contrast ratio	CA: cellulose acetate
CCD: Charge-coupled device	FWHM: Full width at half maximum
1D: One dimensional	GPC: Gel permeation chromatography
2D: Two dimensional	

LIST OF SYMBOLS

\hat{n} : LC director	T : Transmittance
p : Pitch	τ : Turbidity
n_e : Extraordinary refractive index	σ_{avg} : Average cross-section
n_o : Ordinary refractive index	f: frequency
Δn : Optical anisotropy	$I_n(V)$: Intensity of nth order at voltage V
S : Order parameter	V_{pp} : Peak to peak Voltage
$\epsilon_{ }$: Dielectric constant along the long axis of the LC	I_0 : Intensity in the off state
ϵ_{\perp} : Dielectric constant along the short axis of the LC	I : Intensity
ϵ_0 : Free space permittivity	σ_I : Standard deviation of intensity
$\Delta\epsilon$: Dielectric anisotropy	\bar{I} : Average intensity
λ : Wavelength	°C: Degree Celsius
K_{11} : Splay elastic constant	ϵ' : Real part of the dielectric permittivity
K_{22} : Twist elastic constant	ϵ'' : Imaginary part of the dielectric permittivity
K_{33} : Bend elastic constant	$\tan(\delta)$: Dielectric dissipation factor or loss tangent
V_{th} : Threshold voltage	k_B : Boltzmann constant
V_c : Critical voltage	μ : Mobility
	σ : Electrical conductivity